Coupling effect of magnetic polariton in perforated metal/dielectric layered metamaterials and its influence on negative refraction transmission

T. Li, H. Liu, F. M. Wang, Z. G. Dong, and S. N. Zhu

Department of Physics, National Laboratory of Solid State Microstructures, Nanjing University, Nanjing 210093, People's Republic of China
litao@nju.org.cn, zhusn@nju.edu.cn

X. Zhang

5130 Etcheverry Hall, Nanoscale Science and Engineering Center, University of California, Berkeley, California 94720-1740, USA

Abstract: The optical propagation properties and magnetic polariton behaviors in perforated metal/dielectric layered structures are numerically investigated at near-IR region. A developed three-metal-layer (TML) structure is specially inspected as a simple case. Strong coupling effect of magnetic polariton is discovered in this system, which explains why TML structure reveals better negative-refraction property than the reported double-metal-layer (DML) structure. A clear LC-circuit model is presented to describe the physical mechanism of this coupling effect of magnetic polaritons. Detailed results show that the thickness of metal layer influences the transmission greatly and an optimum value is found.

OCIS codes: (240.5420) Polaritons; (260.5740) Resonance; (260.2030) Dispersion; (120.5710) Refraction; (120.7000) Transmission

References and links

1. E. Yablonovitch, "Inhibited spontaneous emission in solid-state physics and electronics," Phys. Rev. Lett. **58**, 2059-2062 (1987).
2. T. W. Ebbesen, H. J. Lezec, H. F. Ghaemi, T. Thio, and P. A. Wolff, "Extraordinary optical transmission through sub-wavelength hole arrays," Nature, **391**, 667-669 (1998).
3. E. Ozbay, "Plasmonic: Merging photonics and electronics at nanoscale dimensions," Science **311**, 189-193 (2006).
4. J. B. Pendry, A. J. Holden, D. J. Robbins, and W. J. Stewart, "Magnetism from conductors and enhanced nonlinear phenomena," IEEE Trans. Microwave Theory Tech. **47**, 2075-2084 (1999).
5. J. B. Pendry, "Negative refraction makes a perfect lens," Phys. Rev. Lett. **85**, 3966-3969 (2000).
6. R. A. Shelby, D. R. Smith, and S. Schultz, "Experimental verification of a negative index of refraction," Science **292**, 77-79 (2001).
7. T. Y. Yen, W. J. Padilla, N. Fang, D. C. Vier, D. R. Smith, J. B. Pendry, D. N. Basov, and X. Zhang, "Terahertz magnetic response from artificial materials," Science **303**, 1494-1496 (2004).
8. T. Koschny and M. Kafesaki, E. N. Economou, and C. M. Soukoulis, "Effective medium theory of left-handed materials," Phys. Rev. Lett. **93**, 107402 (2004).
9. D. R. Smith, J. B. Pendry, and M. C. K. Wiltshire, "Metamaterials and negative refractive index," Science **305**, 788-792 (2004).
10. W. J. Padilla, D. R. Smith, and D. N. Basov, "Spectroscopy of metamaterials from infrared to optical frequencies," J. Opt. Soc. Am. B **23**, 404-414 (2006).
11. A. V. Kildishev, W. Cai, U. K. Chettiar, H. K. Yuan, A. K. Sarychev, V. P. Drachev, and V. M. Shalaev, "Negative refractive index in optics of metal-dielectric composites," J. Opt. Soc. Am. B **23**, 423-433 (2006).
12. S. Zhang, W. Fan, N. C. Panoiu, K. J. Malloy, R. M. Osgood, and S. R. J. Brueck, "Experimental demonstration of near-infrared negative-index metamaterials," Phys. Rev. Lett. **95**, 137404 (2005).
13. V. M. Shalaev, W. Cai, U. K. Chettiar, H. K. Yuan, A. K. Sarychev, V. P. Drachev, and A. V. Kildishev, "Negative index of refraction in optical metamaterials," Opt. Lett. **30**, 3356-3358 (2005).
14. S. Zhang, W. Fan, K. J. Malloy, S. R. Brueck, N. C. Panoiu, and R. M. Osgood, "Near-infrared double negative metamaterials," Opt. Express **13**, 4922-1930 (2005).
15. G. Dolling, C. Enkrich, M. Wegener, C. M. Soukoulis, and S. Linden, "Simultaneous negative phase and group velocity of light in a metamaterial," Science **312**, 892-893 (2006).
16. S. Zhang, W. Fan, K. J. Malloy, S. R. Brueck, N. C. Panoiu, and R. M. Osgood, "Demonstration of metal dielectric negative-index metamaterials with improved performance at optical frequencies," J. Opt. Soc. Am. B **23,** 434-438 (2006).
17. G. Dolling, C. Enkrich, M. Wegener, C. M. Soukoulis, and S. Linden, "Low-loss negative-index metamaterial at

#74651 - $15.00 USD Received 1 September 2006; revised 10 October 2006; accepted 29 October 2006

telecommunication wavelengths," Opt. Lett. **31**, 1800-1802 (2006).
18. S. Zhang, W. Fan, N. C. Panoiu, K. J. Malloy R. M. Osgood, and S. R. J. Brueck, "Optical negative-index bulk metamaterials consisting of 2D perforated metal-dielectric stacks," Opt. Express **14**, 6778-6787 (2006).
19. M. Beruete, M. Sorolla, and I. Campillo, "Left-handed extraordinary optical transmission through a photonic crystal of subwavelength hole arrays," Opt. Express **14**, 5445-5455 (2006).
20. K. J. K. Koerkamp, S. Enoch, F. B. Segerink, N. F. van Hulst, and L. Kuipers, "Strong influence of hole shape on extraordinary transmission through periodic arrays of subwavelength holes," Phys. Rev. Lett. **92**, 183901 (2004).
21. D. R. Smith, D. C. Vier, T. Koschny, and C. M. Soukoulis, "Electromagnetic parameter retrieval from inhomogeneous metamaterials," Phys. Rev. E **71**, 036617 (2005).
22. L. Martin-Moreno, F. J. Garcia-Vidal, H. J. Lezec, K. M. Pellerin, T. Thio, J. B. Pendry, and T. W. Ebbesen, "Theory of extraordinary optical transmission through subwavelength hole arrays," Phys. Rev. Lett. **86**, 1114-1117 (2001).

1. Introduction

Over the last couple of decades, great efforts have been made to control the state of the electromagnetic wave propagation [1-3]. Negative refraction-index material (NIM) is a very hot topic in this field due to its fascinating nature. [4-11]. Recently, NIMs at optical frequency were reported experimentally, which are based on novel designs of the "magnetic atoms" that provide a negative permeability μ [12, 13]. Among these new NIMs, the perforated metal/dielectric sandwich structure was promoted [14] and experimentally verified lately [15-17]. Very recently, a bulk model with stacks of such sandwich blocks was theoretically investigated, exhibiting less loss and better negative refraction properties [18]. At the same time in another report [19], left-handed transmission was demonstrated at microwave region in a similar stacking structure as well. Such results bring exciting news in realizing the useful applicable NIMs.

The propagation of EM wave in the perforated metal-dielectric system can be regarded as a kind of magnetic polariton, which originates from the coupling between EM wave and magnetic resonance. With the contribution of negative ε from the diluted Drude metal, NIM can be achieved artificially. Unfortunately in such a system, electric loss and induction loss inevitably exist, leading to strong absorption and low transmission. Interestingly, the nearest report [18] indicated that the loss could be reduced with more NIM units stacked in wave propagation direction. Although it can be intuitively attributed to the coupling effect of the multiple unit cells, the authors of Ref. [18] did not give a specific explanation on this point. In another recent paper [19], a transmission line model is given to explain the LH extraordinary optical transmission through a photonic crystal of subwavelength holes arrays at GHz region. But this model fails to explain why the transmission loss is reduced when visible light gets through more metal/dielectric layers.

To give a clear view of the underlying physics, we take a three-metal-layer (TML) structure as an example to explore the coupling effect of magnetic polariton. Good comparisons are given between TML and the reported DML. Strong coupling effect is observed in TML system and it results two new eigenmodes: higher frequency symmetric mode and lower frequency antisymmetric mode. Numerical results truly reveal that the symmetric mode exhibits higher negative refraction transmission and lower loss. A coupled LC-circuit model is presented to illustrate the coupling mechanism. Detailed results show the thickness of the metal layer plays a significant role in the magnetic polariton coupling and remarkably affects the medium's optical property. Both the model and the simulation results show that the advantage of TML over DML is realized only in certain thickness range. The best transmission for TML is found at thickness of 40 nm for this concerned circumstance.

2. Numerical models

In order to avoid the complicated influences of the hole shape, which was proved to affect the extraordinary transmissions greatly [20], we construct two typical samples with square holes arrays drilled in the double-metal and three-metal layered structures. Although the reported DML structure with rectangular holes array exhibited optimized property [15-18], the proposed samples with square holes represent a more general consequence. In Fig. 1, a unit cell of the TML structure is given with its geometry size as P=600 nm, a=250 nm, g=20 nm, and the thickness of metal layer t is varied from 20 to 100 nm in simulations. By lacking one metal-layer, the DML sample is designed with the same structural parameters as the TML case.

Finite element numerical method (FEM) is employed in our simulations. Gold is used as the metal material, whose dispersion property is described by Drude model. That is, the effective

#74651 - $15.00 USD Received 1 September 2006; revised 10 October 2006; accepted 29 October 2006

permittivity is given by $\varepsilon=1-\omega_p^2/(\omega^2+i\omega\gamma)$, where the corresponding parameters are taken from Ref. [12] with the plasma frequency $\omega_p= 1.37\times10^{16}$ *rad/s* and scattering frequency $\gamma= 4.08\times10^{13}$ *rad/s*. For simplification, the metal perforated structure is surrounded by air with non-dispersive dielectric coefficient $\varepsilon= 1$. It should be noted that if the gaps between the metal layers are inserted with other non-dispersive dielectrics, the magnetic polariton resonance may shift to some lower frequencies and it does not affect the identical physics.

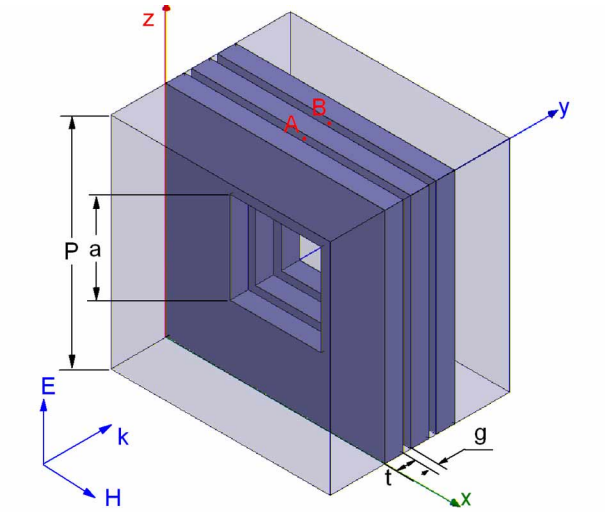

Fig. 1. Unit cell of three-metal-layer structure: the period P=600 nm, hole size a=250 nm, gap between layers g=20 nm, and thickness of metal layer t is changed from 20 to 100 nm in calculations.

As Ref. [19], a theoretical model for normal incidence is developed based on an artificial waveguide with two ideal magnetic conductor vertical planes and two ideal electric conductor horizontal planes at boundaries. It is equivalently valid in an infinite lateral structure with periodic square holes for a polarized incident wave with E-polarization along *z* direction. Then, the light propagating properties can be conveniently obtained by evaluating the S-parameters of the waveguild. Calculations are carried out for the proposed structure as shown in Fig. 1 with incident EM wave propagates along the *y* direction, and also as same as the DML one. As both the lateral period (600 nm) and total thickness (~200 nm) are considerably smaller than the operating wavelength (~1.2 μm), the effective media model is valid in our model. The effective permittivity, permeability and refraction index can be retrieved following the method in Ref. [21].

3. Simulation results and discussions

Firstly, we calculated the transmission properties of DML and TML samples with the thickness of metal layer being 50 nm. The results are shown in Figs. 2(a) and 2(b) respectively. Similar to the results reported before [12], one peak [referred as R0 in Fig. 2(a)] is found at 255 THz in the transmission of the DML structure. As for the TML one, there are two peaks emerging with one blue-shifts to 269 THz [referred as R1 in Fig. 2(b)] and the other red-shifts to 245 THz [referred as R2 in Fig. 2(b)]. Utilizing the method introduced in Ref. [21], the effective electromagnetic coefficients (refraction-index *n*, permittivity ε and permeability μ) of DML and TML structures are retrieved from the simulated S-parameter results, which are presented in Figs. 2(c)-2(h). Although the permeability for both structures does not reach negative, the values of the expression $\varepsilon_1\mu_2+\varepsilon_2\mu_1$, which determines the sign of refraction index [12, 14], can get to negative at some frequency range [shown in Fig. 2(i) and 2(j)]. It is obviously seen that, for both DML and TML cases, negative Re(n) can be obtained at the R0 and R1 peak, respectively. But for TML sample, a sharper peak in the permeability curve (in Fig. 2(f)) is produced at R1 and it means a stronger magnetic resonance occurs. Furthermore, in Fig. 2(d), the peaks in the curves of Re(n) and Im(n) near R1 are closer than those near R0 shown in Fig. 2(c). This results in a higher figure of merit (FOM= |Re(n)/Im(n)|) at R1, which indicates that TML sample has better negative refraction efficiency than DML one. Besides the R1, the additional tiny transmission maximum at R2 for TML sample corresponds to anomalous high positive refraction [see Fig. 2(d)], which would enrich the optical property and potential

#74651 - $15.00 USD Received 1 September 2006; revised 10 October 2006; accepted 29 October 2006

application of TML structure.

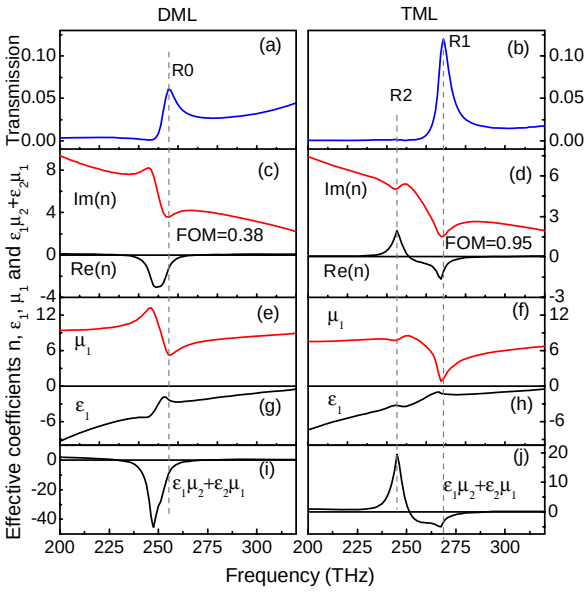

Fig. 2. Transmission spectra and the retrieved effective coefficients of DML structure [(a), (c), (e), (g), (i)] and TML structure [(b), (d), (f), (h), (j)], here ε_1 and ε_2 are the real and imaginary part of permittivity; μ_1 and μ_2 are the real and imaginary part of permeability. In (c) and (d), FOM values are marked out to reveal the transmission efficiency.

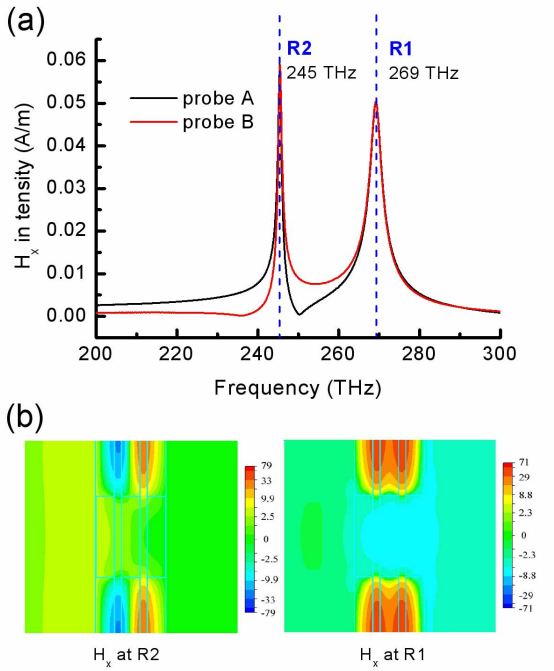

Fig. 3. (a). Detected H_x intensities of TML structure with the frequency ranging from 200 to 300 THz by two probes, which are located at the neighboring layer gaps (marked with A and B in Fig. 1). (b) The corresponding simulated H_x distributions at the frequencies of R1 and R2.

The splitting of magnetic resonance frequency in TML structure is confirmed by detecting the amplitudes of magnetic field H_x at the gaps between two metal layers (as marked with A and B in Fig. 1), which is shown in Fig. 3(a). In relation to the two transmission peaks in Fig. 2(b), there is a great enhancement of localized H field at the two corresponding frequencies. But it is a little surprising

#74651 - $15.00 USD Received 1 September 2006; revised 10 October 2006; accepted 29 October 2006

that though the transmission of R2 is much weaker than R1, its localized H field is even a little stronger than that of R1. To gain an insight, we demonstrate the distributions of magnetic field H_x at the two resonance frequencies, as is given in the Fig. 3(b). The difference between two resonance modes is clearly presented, that the magnetic field H_x in the two gaps oscillates with the same phase at R1 and with anti-phase at R2. Intuitively, the two in-phase oscillations can be regarded as the symmetric magnetic polaritons, which enhance the reversed magnetic field resulting in a deep dip in the μ dispersion [see Fig. 3(f)]. While the anti-phase polaritons counteract each other, thus contributes little to the permeability. From another point of view, for R2 case, two anti-pahse magnetic dipoles can be seen as a magnetic quadrupole, whose radiation ability is much weaker than the two synchronal dipoles (R1 case). As well as Ebbesen defined "plasmon molecule" [22], we may call the coupling modes as "magnetic polariton molecule" with a level split.

So far, two magnetic polaritons coupling is well exhibited. It is undoubtedly believed that the coupling of more polaritons in multi-structures will show more complicated and interesting features. But in the present work, our attention is mainly focused on the detailed coupling property of the two-polaritons system (TML), and to seek the most important factor in such coupling. It also should be mentioned that, quite different from Ref. [18], in which the structure is only a stack of multiple unit cells, our TML structure is still a unit cell. So their coupling manners are not the same, though the superiority brought from the multiple metal layers is somewhat similar. To better understand the coupling effect and the resonance split, an equivalent LC-circuit model is constructed by introducing the concepts of "effective self inductance and mutual inductance". From Pendry's theory, the metal part at high frequency can be regarded as an effective inductance L_m, which can be derived from the effective impedance $Z_{metal}=i\omega L_m$. For our modeled structure, Z_{metal} can be calculated from effective capacitor C_m for the metal surface as

$$Z_{metal}=\frac{1}{i\omega C_m}=\frac{1}{i\omega\varepsilon_m\frac{\varepsilon_0 S}{l}}=-i\frac{l}{\omega\varepsilon_0 S}\frac{1}{(1-\frac{\omega_p^2}{\omega^2})}\approx i\omega\frac{l}{\omega_p^2\varepsilon_0 S}, \tag{1}$$

where S and l are the cross-section area and length of the conductor, respectively. So L_m is deduced as

$$L_m=\frac{l}{\omega_p^2\varepsilon_0 S}=\frac{1}{\omega_p^2\varepsilon_0}\frac{P-a}{at_{eff}}. \tag{2}$$

Here, the structure parameters P and a are already given in Fig. 1, and t_{eff} is the effective thickness of the surface current layer. Because the distribution of alternating electric field penetrated into the metal is not homologous, as is dominated by the "skin depth" d_s, the induced current also distributes in an effective region inside the metal. As the total current can be integrated from the d_s-dependent current density, effective thickness is thus obtained with the exponential form

$$t_{eff}=d_s(1-\exp(-t/d_s)). \tag{3}$$

Substituting Eq. (3) to Eq. (2), the effective inductance is achieved. Equivalent to the resonant LC-circuit, the resonant frequency of a single magnetic polariton in the proposed DML structure should have the form

$$\omega_0=\frac{1}{\sqrt{L_m C}}\propto\left(1-\exp(-t/d_s)\right)^{1/2}. \tag{4}$$

Notice that, the skin depth (d_s) is important both in the single magnetic resonance and the coupling behavior, which will be emphasized later.

When two magnetic polaritons couple together, the system can be described as two coupled resonant LC-circuits, whose effective inductance changes depending on the symmetry of coupling currents. As Fig. 4 illustrates, the symmetric mode of the magnetic polariton corresponds to the anti-phase current flows in the coupled part, which results in a reduced effective inductance L_m-M. Here M is an effective mutual inductance between two coupled circuits, which is determined by the coupling strength. Whereas the antisymmetric mode induced by the in-phase current flows corresponds to an increased inductance L_m+M. Thus the original single resonance ω_0 splits into two new frequencies

$$\omega_{R1}=\frac{1}{\sqrt{(L_m-M)C}},\quad \omega_{R2}=\frac{1}{\sqrt{(L_m+M)C}}, \tag{5}$$

#74651 - $15.00 USD Received 1 September 2006; revised 10 October 2006; accepted 29 October 2006

for the symmetric and antisymmetric modes respectively. Apparently, the split resonances with the red and blue shifts to the original ω_0 are presented in a compact form. It phenomenologically agrees with above simulated results. As the mutual inductance is approximately considered mainly from the two near-paralleled surface currents, the magnitude of *M* should be in inverse proportion to the currents distance, which depends mostly on the layer thickness.

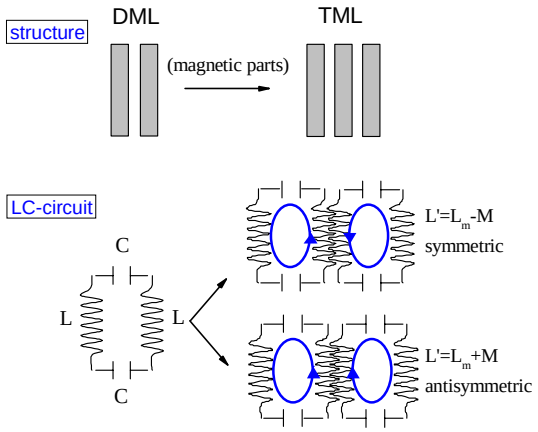

Fig. 4. Schematics of the equivalent LC-circuit models corresponding to the magnetic structures of DML and TML cases.

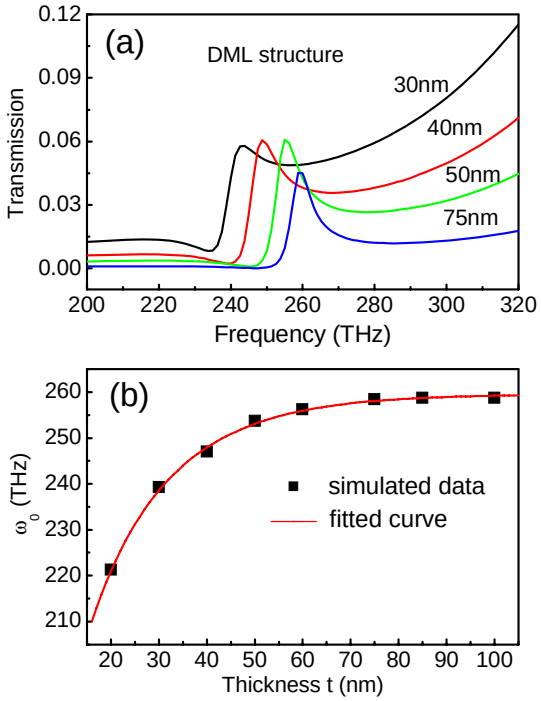

Fig. 5. (a). Transmission spectra of DML structure with various layer thickness (t= 30, 40, 50, 75 nm). (b) Resonance frequency ω_0 of peak R0 as a function of layer thickness. The symbols are the simulated data and the red curve is the fitted result by Eq. (4).

From the above LC-circuit model, we find that the thickness of metal layer plays a significant role in both the single magnetic resonance and the coupling effect. Consequently, series of DML and TML samples with the layer thickness ranging from 20 to 100 nm are simulated in the following. Figure 5(a) exhibits the transmission spectra of four DML structures with t=30, 40, 50, and 75 nm

#74651 - $15.00 USD Received 1 September 2006; revised 10 October 2006; accepted 29 October 2006

for examples. It is obviously seen that transmission peak shifts to lower frequency with decreasing the thickness of metal layer. Resonant frequency ω_0 of the single magnetic polariton as function of the layer thickness t is plotted in Fig. 5(b), revealing an increasing dependence. According to Eq. (4), a good fit is achieved and it gives the value of the skin depth as d_s=17.5 nm. Convincingly, the exponential curve indicates the strong influence of the skin depth.

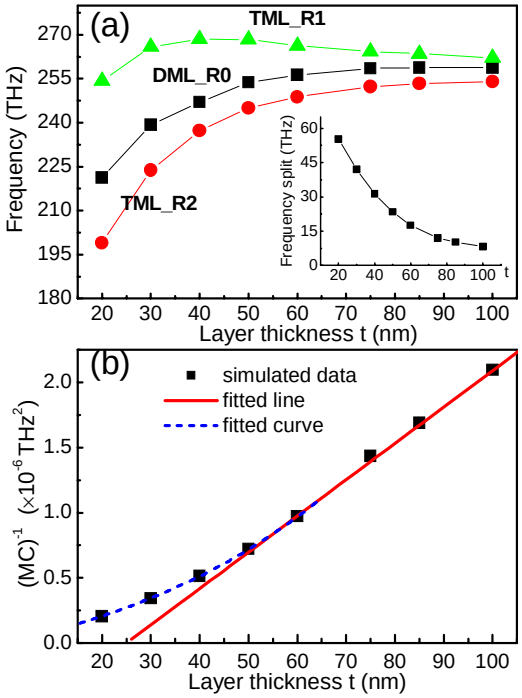

Fig. 6. (a). Splitting frequencies (ω_{R1} and ω_{R2}) of TML structure as functions of the layer thickness accompanied with the frequency (ω_0) of DML one for comparison. Inset displays the frequency split (ω_{R1}- ω_{R2}) versus the layer thickness. (b) The calculated value of $(MC)^{-1}$ with respect to the layer thickness. The symbols are the data derived from the simulated frequencies by Eq. (6), and the red line is a linear fit with respect to data at large t region while the dashed blue curve is fitted by exponential relation based on the small t data.

Subsequently, two resonance frequencies of TML structure versus the layer thickness are shown in Fig. 6(a) with a comparison to the DML case, and the inset plots the splitting intensities. One can clearly observe that, with the layer thickness increasing, the frequency split reduces and two branches (R1 and R2) of TML tend to degenerate to the R0 of DML. However, for the upper branch, the change tendency of resonant frequency is not a monotonous relation to t, but exhibits a maximum at about t=40 nm. Compared with the curve shape of DML_R0, we can undoubtedly attribute it to the influence of the t-dependent self-inductance (L_m). To make a detailed inspection, amplitude of mutual inductance M is evaluated, which can be extracted from the simulated split frequencies ω_{R1} and ω_{R2} by Eq. (5), as

$$MC = \frac{1}{2}\left(\frac{1}{\omega_{R2}^2} - \frac{1}{\omega_{R1}^2}\right). \tag{6}$$

Because the capacitance C is considered unchangeable for the fixed layer gaps, M can be evaluated from Eq. (6). Symbols in Fig. 6(b) are the extracted $(MC)^{-1}$ values corresponding to the various layer thickness t. As we can see, at large t region $(MC)^{-1}$ truly has a linear relation to t with the form of $(MC)^{-1}= k(t\text{-}25)$ as the red fitted line shows. However, the $(MC)^{-1}$ data diverges from the straight line as t decreases. This fact indicates that the proposed "surface current" induced mutual inductance by interacted magnetic field is only valid for the large t cases. It can be understood as follows: For the thick-layer structures, the surface currents mostly concentrate within the skin depth region, and can be considered as isolated current elements with an effective distance $r= t\text{-}25$ nm, where M is dominated by the mutual magnetic field which scales reciprocal to the distance r; When t becomes

#74651 - $15.00 USD Received 1 September 2006; revised 10 October 2006; accepted 29 October 2006

smaller, the currents tend to interact directly hence the overlap of currents appears more and more prominent. The fitted curve on $(MC)^{-1}$ data at the small t region indicates an exponential growth relation to the layer thickness, as the dashed blue curve in Fig. 6(b) displays, which suggests the M can be attributed to the specific current distributions and intensities caused by the currents overlapping. Although accurate mathematical form of M is not given here, the equivalent "mutual inductance" model phenomenologically provides a concise and effective description on the coupling of two magnetic polaritons.

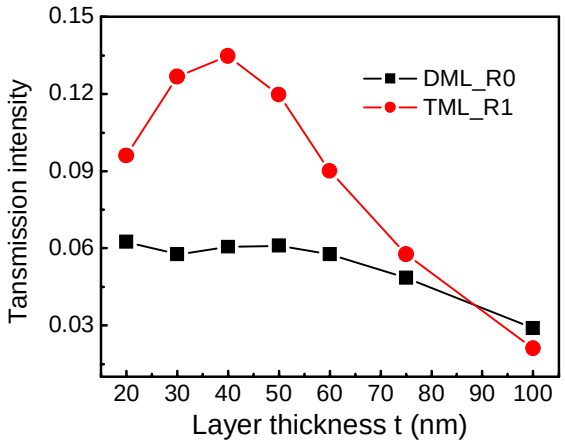

Fig. 7. Transmission intensities of peak R0 and R1 versus the layer thickness for the DML and TML structures, respectively.

More importantly, our simulations exhibit another striking aspect that the transmission enhancement of TML structure is modulated by the layer thickness. Fig. 7 displays the peak intensities of the R0 and R1 versus the layer thickness for the DML and TML structures respectively. An enhancement maximum can be found at t=40 nm, which is about two times the skin depth (d_s=17.5 nm). When the layer thickness is above 85 nm, the intensity of R1 is weaker than that of R0, which reveal a fact that the transmission advantage of TML over DML disappear at large thickness region. In other words, the optimization of the TML sample for lower loss only exists in a limited range confined by the metal layer thickness. To highlight the physical mechanism, one can imagine the symmetric mode for TML structure, which is actually excited by the anti-phase current flows on both surfaces of the middle layer, as schemed in Fig. 4. Thus it is reasonable that, when $t>2d_s$ the electrons in the midst of the middle layer can hardly be excited and remain a "static state", which depresses the resonance efficiency and hampers the energy flow. As the layer thickness increases, these "static" electrons increase in amount as well, so more energy is blocked and the transmission is enhanced less and less, even to be weakened when t>85 nm. On the other hand, if $t<2d_s$, the two anti-phase skin currents are overlapped and tend to trail off, which suppresses the in-phase magnetic resonance and also leads to a decline of the transmission. Therefore, a highest enhancement is reached at $t=2d_s$, where the most efficient symmetric coupling occurs. Hence a best condition is provided to improve the negative refraction transmission.

Now, we realize that although for most cases TML structure appears better negative refraction property with lower loss, the optimization actually depends on the thickness of the metal layer associated with the skin depth of the metal. The best transmission condition is found that the layer thickness is about two times the skin depth ($t=2d_s$), which is numerically demonstrated and agrees well with the proposed LC-circuit model. By the way, it should be mentioned that same simulation processes and analyses are performed in the optimized DML and TML structures with rectangular holes. Similar results about the coupling effect are obtained, only with the changed resonance frequencies and increased FOM values. The criterion of the layer thickness provides us an instruction in the design of the low loss NIMs. It goes beyond the discovery of the report in Ref. [18]. Our result also explains why the transmission enhancement did not take place in the experimental report in Ref. [19]. Because their metal layer thickness is much larger than the skin depth in the GHz

#74651 - $15.00 USD Received 1 September 2006; revised 10 October 2006; accepted 29 October 2006

region, which is far beyond the advantageous range for the multi-metal-layer system. Additionally, we have also investigated more metal-layered systems, the coupling modes become more complicated and will be discussed elsewhere; nevertheless the importance of the layer thickness is identical. In fact, the coupling effect of the magnetic polariton in TML structure is the fundamental coupling, as is considered as two quasi-particles interaction. Its scientific significance is the reason why we emphatically stressed all through the context.

4. Conclusions

In conclusion, the properties of magnetic polariton in double-metal-layer and three-metal-layer structures with perforated holes array are numerically studied and compared in detail. Two new resonance modes are discovered in three-metal-layer structure, symmetric mode at higher frequency and antisymmetric mode at lower frequency, which come from the splitting of the single mode of double-metal-layer structure due to the coupling effect between two magnetic resonances in neighboring gaps. The retrieved effective refractive index shows the symmetric mode possesses better negative refraction property with lower loss for certain metal layer thickness. A phenomenological LC-circuit model based on the effective inductance is proposed to explain the resonance behaviors of single and coupled magnetic polaritons. Simulation results indicate the thickness of metal layer is a key factor to determine the optical property of metamaterial. The best transmission enhancement of the TML structure with respect to the DML one is obtained at an appropriate thickness (t~$2d_s$), which presents an optimized structural design of NIM. From the results reported in this paper, it is noticeably shown that the magnetic coupling effect is very important in the negative refractive properties of perforated metal/dielectric layered system. Actually, in many other metamaterial systems, such a magnetic coupling mechanism should be taken into consideration and new interesting properties are expected.

Acknowledgments

This work is supported by the National Natural Science Foundations of China under contract No. 10534042, No. 60578034 and No.10523001.

#74651 - $15.00 USD Received 1 September 2006; revised 10 October 2006; accepted 29 October 2006